UDC 621.74.043:669.71'782

CRYSTALLIZATION CONDITIONS AND STRUCTURE OF Al – Si ALLOYS IN CASTING UNDER PRESSURE

L. V. Nikulin[1]

Translated from Metallovedenie i Termicheskaya Obrabotka Metallov, No. 9, pp. 21 – 25, September, 1997.

The Al – Si system comprises widely used castable aluminum alloys. The structure of these alloys has been studied in many works but its special features in pressure casting have not been described sufficiently well. The present work is devoted to the crystallization conditions in pressure casting and an analysis of the structure of Al – Si alloys.

The special features of Al – Si alloys cast into one-time and chill molds have been considered in detail in [1, 2]. However, we cannot say that alloys of the Al – Si system have been studied sufficiently well. For example, after special casting technologies with the use of high-pressure alloys the system contains structural components with an as yet unknown morphology. This refers to casting under pressure. Despite the fact that the process has been known from the beginning of the century there are virtually no works devoted to a detailed analysis of the crystallization mechanism and the kinetics of the alloys under these conditions. Photographs of microstructures of Al – Si alloys presented in [2, p. 471], [3, p. 33], [4, p. 141] do not reflect the structure to a full extent. However, it is known that the structure of alloys cast under pressure is characterized by a well-defined difference in the grain sizes [2, p. 484].

We studied aluminum alloys containing 8.2 and 18.3% Si. The alloys were fabricated in a resistance furnace from aluminum A99 and a binary Al – 24% Si alloying set without modification. Specimens with the size of the functional part equal to 3 × 20 × 60 mm were prepared by casting under pressure in a 711A08 machine that provides a pressure of at most 100 N/mm^2 on the metal in the crystallization period.

The structure of the alloys is represented by primary segregations of an α-phase (Fig. 1*a*) or β-solid solutions and an eutectic (Fig. 1*b*). A metallographic analysis has shown that the sizes of the primary segregations of both α- and β-phases scatter substantially. Before analyzing the kinetics of the process we had to determine whether this difference in the sizes was a consequence of the dissection of dendrite axes of increasing orders by the plane of the microscopic specimen or if we had to deal with different crystal families.

The data of a statistical analysis have shown (Fig. 2) that all the measured sizes of the α-phase segregations can be divided into two groups. The maxima of the distribution curves were shifted over the axis of abscissas by several tens of micrometer. Thus, the structures of the alloys had two groups of crystals formed in different periods of time.

Let us analyze the temperature and dynamic conditions of the appearance of such a structure. It is assumed that silumins, which are narrow-range alloys, crystallize gradually due to the high rate of their cooling. Let us evaluate the temperature drop in casting alloy Al – 8.2% Si with a thickness of 3 mm into a mold from steel 30Kh5MFS [the coefficient of heat accumula-

[1] Research Institute of Powder Technology and Coatings, Perm, Russia.

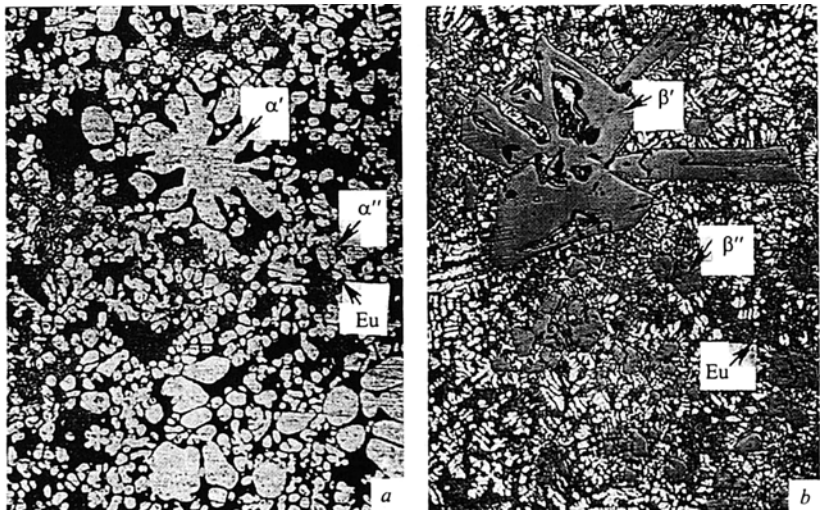

Fig. 1. Microstructure of hypoeutectic (*a*) and hypereutectic (*b*) alloys (a Neophot-21 microscope, × 320).

0026-0673/97/0910-0384$18.00

tion of the steel $b_f = 12{,}270$ W · sec$^{1/2}$/(m^2 · K)] [5, p. 183]. In accordance with [1, p. 9] the crystallization range of the alloy is 620 – 577 = 43°C. We will use the capacity of the Biot criterion of the intensity of thermal interaction to include physical and geometrical characteristics of the body participating in the heat exchange and to reflect the proportion of the temperature drop in the cross section of the body to the temperature head[2] on its surface, namely,

$$\mathrm{Bi} = \frac{\alpha \delta_{cast}}{\lambda_l} = \frac{T_{lc} - T_{ls}}{T_{ls} - T_{2s}}, \quad (1)$$

where α is the coefficient of heat transfer from the surface of the casting, W/(m^2 · K); δ_{cast} is the thickness of the casting, m; λ_l is the thermal conductivity of the material of the casting, W/(m · K); T_{lc}, T_{ls} are the temperatures in the center and on the surface of the casting, K; T_{2s} is the temperature on the surface of the press mold, K.

In the process of heat transfer the Biot criterion changes; the heat transfer coefficient α decreases with the heating of the press mold. In addition, with the change in the state of aggregation of the metal of the casting its thermal conductivity changes too. A calculation of the thermal conductivity of alloy Al – 8.2% Si from the thermal conductivities of aluminum and silicon above and below the melting point of aluminum with the use of the data of [6, p. 86] and [7, p. 183] has shown that in a liquid state $\lambda_l = 90.96$ W/(m · K) and in a solid state $\lambda_l = 203.1$ W/(m · K). Thus, in the process of crystallization the thermal conductivity of the alloy changes by more than a factor of 2.

The results of a calculation of the temperature drop in a casting in the beginning of crystallization (at $\tau = 0.04$ sec) and in the end of it ($\tau = 0.16$ sec) with the use of relation (1) are presented in Table 1. We assumed that in the beginning of the crystallization process $T_{ls} = T_{liq} = 620$°C and in the end $T_{ls} = T_{sol} = 577$°C, where T_{liq} and T_{sol} are the liquidus and solidus temperatures, $T_{2s} = 442$ and 517°C (the temperatures of the beginning and end of heating of the press mold respectively). The results of the calculation show that the temperature drop in the body of the casting decreases by an order of magnitude during 0.12 sec. The temperature field levels off due to the further heating of the surface of the press mold by the crystallization heat and the resulting increase in the contact temperature. However, the principal role is played by the rapid fall of the temperature in the center of the casting.

[2] The difference in the temperatures of the surfaces of the casting and the press mold.

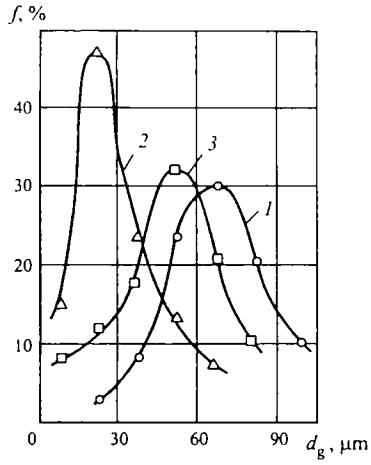

Fig. 2. Curves of the size distribution cross sections of the structural components of alloy Al – 8.2% Si: 1) α′-dendrites; 2) α″-dendrites, 3) eutectic regions.

The nature of the crystallization, i.e., gradual or bulk, was determined from the approximate relation

$$T_{liq} - T_{sol} = \frac{b_f/\sigma_l}{T_{lc} - T_{ls}}. \quad (2)$$

In the beginning of the process the crystallization range (43°C) of the alloy (Al – 8.2% Si) was below the value $\frac{12{,}270}{15{,}400} \times 152.6 = 121$°C. By the end of the process we had $\frac{12{,}270}{24{,}600} \times 15.1 = 7$°C, which is several times lower than the range of the crystallization temperature. Thus, the conditions for gradual crystallization exist in the initial stage, whereas in the rest of the time the narrow-range alloy Al – 8.2% Si cast under pressure crystallizes over the whole volume of the casting.

The pressure of the hydraulic impact and of premolding is transferred into the mold not instantaneously but after 0.12 – 0.14 sec [8, p. 14]. The effect of the pressure on the crystallizing metal can influence the process of formation of structural components as a result of the change in the liquid-

TABLE 1

Stage of the process	Thermophysical properties			b_f, W · sec$^{1/2}$/(m^2 · K)	α, W/(m^2 · K)	Bi_l	$T_{lc} - T_{ls}$, K
	λ_l, W/(m · K)	C_s, J/(kg · K)	ρ, kg/m^3				
Initial ($\tau = 0.04$ sec)	92.96	2.36	1090.7	15.46	34,660	1.13	152.6
Final ($\tau = 0.16$ sec)	203.1	2.51	1214.0	24.87	17,330	0.256	15.1

Note. The characteristics were calculated by the formulas $b_f = \sqrt{\lambda c \rho}$; $\alpha = \frac{b_f}{\sqrt{\pi \tau}}$; $\mathrm{Bi} = \frac{\alpha \delta_{cast}}{\lambda_l}$; $T_{lc} - T_{ls} = \mathrm{Bi}_l (T_{ls} - T_{2s})$.

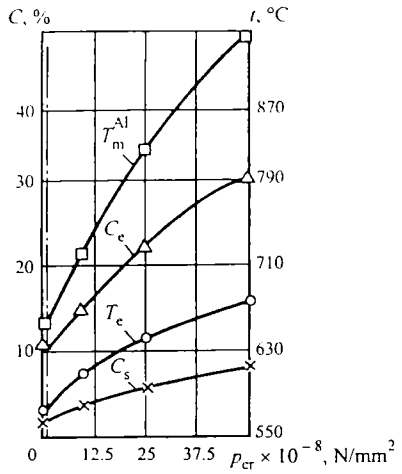

Fig. 3. Effect of the pressure in crystallization on the position of critical points of the Al – Si diagram (by the data of [12]). The vertical dash line corresponds to a pressure of 100 N/mm^2.

phase diffusion, the coefficient of distribution of silicon, and the conditions of nucleation. The diffusion and self-diffusion in metallic melts occurs by a "hole" mechanism [9, p. 193 – 195]. The dependence of the diffusivity on the external pressure for metals is expressed by the formula [10, p. 114]

$$d(\log D) = \frac{\Delta V}{kT}, \qquad (3)$$

where ΔV is the relative reduction of volume in compression. In accordance with [11, p. 23], the compressibility of aluminum in a liquid state at the melting temperature is equal to 20 m^2/GN. A calculation of the relative compression at a pressure of 100 N/mm^2 has shown that the linear sizes of any specified volume decrease by 0.2%. The decrease in the distance between the particles of the liquid by 0.2% does not change the hole mechanism of the mass transfer and hence does not affect the conditions of the arrival of silicon and aluminum atoms at the crystallization front.

Using the data of [12, p. 123] for the Al – Si diagram we plotted the dependences of the melting temperature of pure aluminum T_m^{Al} and the eutectic T_e, the concentration at the maximum solubility C_s, and the eutectic point C_e on the pressure applied in the crystallization process (Fig. 3). At a pressure of 100 N/mm^2 the changes in the diagram are low and we have no reason to think that the effect of the change in the distribution coefficient on the results of the formation of α- and β-crystals is significant.

The effect of the growth of the melting temperature of aluminum (by about 6 K) should be treated as significant. Nonmodified Al – Si alloys crystallize when overcooled by 0 – 4 K [10, p. 270] and therefore a sudden elevation of the equilibrium crystallization temperature above the actual hardening temperature of the aluminum melt should stimulate the nucleation of primary crystals.

In order to determine the specific features of the structure formed under the conditions of pressure casting the Al – 8.2% Si alloy was also crystallized in a mold under a pressure of 100 N/mm^2 created by a piston (an ingot 40 mm in diameter and 70 mm high). The structure of the alloy crystallized under the same pressure at different cooling rates is shown in Fig. 4. Under the chosen magnification (× 80), dendrite formations are observed clearly, which makes it possible to estimate the sizes of micrograins. We measured the length (l_t) and thickness (b_t) of trunks of coarse and fine dendrites and the length and thickness of branches of the second order (l_b and b_b). Branches of the third order in dendrites of alloys crystallized by the method of pressure casting and pressed by a piston were not observed. We measured the sizes of eutectic regions in two mutually perpendicular directions. The number of structural fragments N_V in a unit volume of 1 mm^3 was determined from the mean size $\bar{b}$ (predominantly the length) and the number of studied fragments N_a on an area of the metallographic specimen.

The calculation was conducted by the formula [13, p. 80]:

$$N_V = \frac{N_a}{\bar{b}}. \qquad (4)$$

The results of the measurements are presented in Table 2.

The mean size of coarse dendrites in the pressure-cast alloy is almost half of that in the alloy crystallized under the pressure of a piston; the sizes of the cross sections of branches are a factor of 2.5 – 3 less. The alloy hardened under the action of the piston did not experience a separate pressure pulse and therefore its structure is devoid completely of the zone of fine dendrites; the eutectic component forms a continuous matrix.

The results of the measurements can be used for estimating the cooling rate of aluminum alloys in pressure casting. In accordance with the dependence of the grain size on the cooling rate presented in [11, p. 45], the cooling rate is on the average 100 °/sec at a distance of 6 – 12 μm between secondary dendrite branches.

The crystallization process in pressure casting occurs in the following order. After the metal fills

TABLE 2

Fragments of the structure	l_t, μm	b_t, μm	l_b, μm	b_b, μm	N_V, mm^{-3}	V_s*
Casting under pressure						
Coarse dendrites	207 ± 20	10.25 ± 0.8	46 ± 6.0	12 ± 1,5	74	0.08
Fine dendrites	62.5 ± 12	13.75 ± 0.9	16.5 ± 3.0	6.2 ± 0.5	8640	0.59
Eutectic regions	147 ± 10	27.5 ± 3.5	–	–	1600	0.33
Crystallization under pressure of a piston						
Coarse dendrites	400 ± 33	22.5 ± 3.5	60.5 ± 13	30 ± 3.2	15	0.35
Eutectic	Continuous matrix				–	0.65

* V_s is the proportion of structural components.

the press mold, when a considerable temperature gradient is created in the casting, individual dendrites of the α′-phase appear and grow, attaining a considerable size by the end of the crystallization. In the subsequent rapid fall of the temperature at the center of the casting new dendrites appear and develop. The concentration of silicon in the liquid surrounding the dendrites increases and the temperature of the beginning of the equilibrium crystallization of the liquid decreases. After a period $\tau = 0.12 - 0.14$ sec the high-pressure pulse reaches the hardened metal in the press mold and initiates an avalanche nucleation of numerous fine crystals of the α″-phase. X-ray microscopic spectral analysis has shown that the composition of the internal layers of coarse dendrites (α′) contains $0.86 \pm 0.28\%$ Si on the average, whereas fine dendrites (α″) contain $1.40 \pm 0.21\%$ Si.

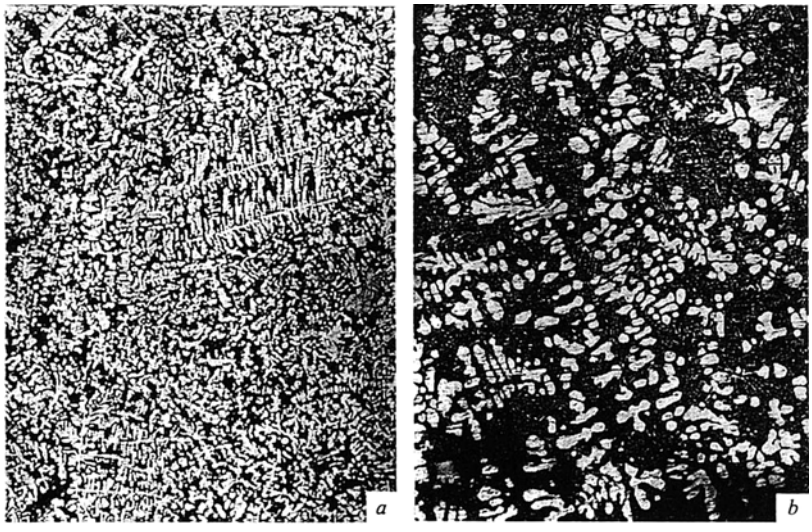

Fig. 4. Macrograins in alloy Al – 8.2% Si crystallized by pressure casting (*a*) and under the pressure of a piston (*b*), × 80.

The formation of another crystal system hampers but does not stop the growth of the initially formed dendrites. The position of crystals of the new system coincide in space with the volumes of the melt not touched by segregation; in these volumes the degree of supercooling caused by the pressure pulse is higher. The building material is insufficient for the development of a spatial structure of fine dendrites; due to the large number of fine crystals the proportion of the solid phase precipitated on each of them is not high. The formation of fine dendrites enriches the mother solution additionally with silicon atoms and the crystallization process is further realized by the eutectic mechanism. The transition to the stage of eutectic crystallization stops the growth of dendrites and fixes the difference in sizes that exists at the moment.

The number and sizes of the volumes for crystallization of the eutectic are controlled by the presence of unoccupied interdendrite spaces. In this connection, the position of the eutectic component in the structure obeys the orientation of primary α′ and α″ dendrites. As a result, the structural components of the alloy form colonies having a constant composition, structure, and size (Fig. 5). A coarse dendrite is positioned in the center of a colony and surrounded by a corona of fine dendrites separated by eutectic regions. A hypereutectoid alloy has a similar structure, namely, β′ and β″ excess crystals of the solid solution and an eutectic (see Fig. 1*b*).

It is expedient to depict the kinetics of the process using Tamman's curves [14, p. 43]. However, it is hardly possible to relate correctly the rate of appearance of crystallization centers n and the linear growth rate c with the degree of supercooling ΔT; in the crystallization process ΔT either decreases or increases, or can become zero depending on the simultaneous variation of the cooling rate, the concentration of the second component in the liquid phase, and the level of the pressure exerted on the metal. The relationship of the mentioned factors to the length of the process can be estimated

Fig. 5. Structure of a crystal colony in alloy Al – 8.2% Si (a diagram): *1*) α′-dendrite; *2*) α″-dendrites; *3*) eutectic regions.

more reliably. Data on the actual values of n [mm^{-3}] and c [mm/sec] are obtained from a statistical analysis of the structural components.

Let us consider the possibilities for analyzing the parameters n and c using the curve describing the size distribution of grains. In volume hardening the largest α-crystals nucleate in the beginning of the process and grow during the entire crystallization time of the α-phase, i.e., until the eutectic crystallizes. On the contrary, the finest α′ and α″ crystals appear directly before the beginning of crystallization of the eutectic.

Figure 6 presents the correlation between the number of crystals n and the time of the process τ_{cr} plotted in the following way. The sizes of macrograins are plotted over the axis of abscissas in order of decreasing sizes beginning with

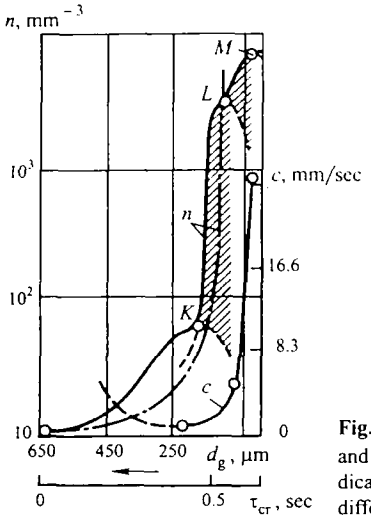

Fig. 6. Kinematic curves $n = f(\tau_{cr})$ and $c = f(\tau_{cr})$ (the hatched areas indicate regions where the amounts of different crystals were summed).

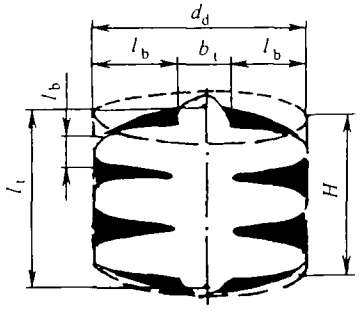

Fig. 7. Diagram for calculating the linear growth rate of crystals.

the maximum one. The initial and the final parameters of macrograins over the axis d_g are matched with the corresponding values of the time of the process over the axis τ_{cr}.

The segment OK of the curve reflects the stage of growth of coarse dendrites followed by a rapid growth of the total number of crystals due to the inclusion of fine dendrites into the crystallization process (segment *KL*). The process commences (region *LM*) with hardening of the eutectic. The successive set of these segments is approximated quite well by an exponential curve (the dash-and-dot line in Fig. 6) typical for crystallization processes. In this connection, we can assume that on the whole the curve *OM* reflects adequately the actual situation. It should be noted that the number of crystals should be laid off on the ordinate axis rather than their fraction. The matching of the time interval of the crystallization and the sizes of the macrograins makes it possible to obtain data on crystal sizes at any moment of time and calculate the rates of their growth. Such calculations are correct because the growth rate of the dendrites does not depend on supercooling [15, p. 124] but is closely related to the amount of crystallization heat removed in each time interval.

Let us calculate the linear rate of crystal growth. We assume that the crystallization time τ_{cr} of each individual structural component (conventionally independent of the crystallization time of the other components) is directly proportional to its volume fraction V_c in the structure (Table 2). Then the volume of the solid phase V_s (in mm³/piece) precipitated in a unit time on a single crystal can be determined by the formula

$$V_s = \frac{V_c}{N_V} \tau_{cr} . \qquad (5)$$

We assume that the volume of the metal contained in the body of the dendrite can be calculated as the volume of a cylinder with a diameter d_d equal to the sum of the lengths of two branches and the thickness of the trunk (Fig. 7). Then the running value of the height of the cylinder can be equated to the length of the trunk changing in the crystallization process. By dividing V_s by the area of the base of the dendrite cylinder S we obtain the increment of the length in mm/sec, i.e., the value of c. The results of the calculation are presented in Table 3.

The data obtained in the measurement of the size of a macrograin and the determination of the total number of grains were used as reference points for plotting segments of the kinetic curve describing the rate of appearance of crystallization centers n; the calculated growth rates were used as reference points for plotting the curve of the linear growth of c (Fig. 6).

TABLE 3

Structural components	τ_{cr}, sec	$V_{sol} \times 10^4$, mm³/piece	$S \times 10^5$, mm²	c, mm/sec
Coarse dendrites	0.08	140	8	1.75
Fine dendrites	0.59	1.1	0.2	5.5
Eutectic	0.33	6.25	0.2	30.53

Notation: τ_{cr} is the reference crystallization time; V_{sol} is the specific volume of the solid phase; S is the area of dendrite base; c is rate of the growth of the structural component in crystallization of alloy Al – 8.2% Si.

CONCLUSIONS

1. The special features of heat exchange between the casting and the press mold in pressure casting create conditions for a predominant crystallization in Al – Si alloys by a volume mechanism.

2. One of the main causes of the marked difference in the grain sizes of the structure of aluminum alloys cast under pressure is the high-pressure pulse that stimulates the formation of numerous fine crystals around the earlier grown dendrites.

REFERENCES

1. G. B. Stroganov, V. N. Rottenberg, and G. B. Gershman, *Aluminum-Silicon Alloys* [in Russian], Metallurgiya, Moscow (1977).
2. L. F. Mondolfo, *Structure of Aluminum Alloys* [Russian translation], Metallurgiya, Moscow (1979).

3. A. K. Belopukhov, M. B. Bekker, M. L. Zaslavskii, et al., *Pressure Casting. 2nd Ed.* [in Russian], Mashinostroenie, Moscow (1975).
4. M. B. Bekker, *Pressure Casting. 3rd. Ed.* [in Russian], Vysshaya Shkola, Moscow (1976).
5. I. I. Goryunov, *Press Molds for Pressure Casting. A Reference Book* [in Russian], Mashinostroenie, Leningrad (1973).
6. V. E. Zinov'ev, *Thermophysical Properties of Alloys at High Temperatures* [in Russian], Metallurgiya, Moscow (1989).
7. G. V. Samsonov (ed.), *Properties of Elements, A Reference Book* [in Russian], Metallurgiya, Moscow (1976).
8. A. K. Belopukhov, E. M. Rodionov, M. L. Zaslavskii, et al., *Pressure Casting. Premolding Problems* [in Russian], Mashinostroenie, Moscow (1971).
9. Ya. I. Frenkel, *Introduction to the Theory of Metals* [in Russian], GNTI, Moscow – Leningrad (1948).
10. R. W. Cahn (ed.), *Physical Metallurgy, Vol. 2* [Russian translation], Metallurgiya, Moscow (1987).
11. J. E. Hatch (ed.), *Aluminum. The Properties and Physical Metallurgy* [Russian translation], Metallurgiya, Moscow (1989).
12. A. Ya. Shinyaev, *Phase Transformations and Properties of Alloys under High Pressure* [in Russian], Nauka, Moscow (1973).
13. K. S. Chernyavskii, *Stereology in Metal Science* [in Russian], Metallurgiya, Moscow (1977).
14. A. P. Gulyaev, *Metal Science* [in Russian], Metallurgiya, Moscow (1986).
15. G. F. Balandin, *Formation of the Crystal Structure of Castings* [in Russian], Mashinostroenie, Moscow (1973).